Emergent flat band lattices in spatially periodic magnetic fields

M. Tahir,[1] Olivier Pinaud,[2] and Hua Chen[1,3]

[1] *Department of Physics, Colorado State University, Fort Collins, CO 80523, USA*
[2] *Department of Mathematics, Colorado State University, Fort Collins, CO 80523, USA*
[3] *School of Advanced Materials Discovery, Colorado State University, Fort Collins, CO 80523, USA*

Motivated by the recent discovery of Mott insulating phase and unconventional superconductivity due to the flat bands in twisted bilayer graphene, we propose more generic ways of getting two-dimensional (2D) emergent flat band lattices using either 2D Dirac materials or electron gas (2DEG) subject to moderate periodic magnetic fields with zero spatial average. We find that 2DEG shows recurring "magic" values of the magnetic field when the lowest band becomes flat, while for Dirac electrons the zero-energy bands are asymptotically flat without magicness. We explain these nontrivial behaviors using minimal tight-binding models on a square lattice inspired by the Wannier functions of the flat bands, and find that the magicness of the 2DEG is due to destructive quantum interference similar to classic flat-band lattice models. The two cases can be interpolated by varying the g-factor or effective mass of a 2DEG, which also leads to flat bands with nonzero Chern numbers for each spin. Our work provides flexible platforms for exploring interaction-driven phases in 2D systems with on-demand superlattice symmetries.

Introduction— Moiré structures formed by stacking 2D crystals such as graphene, hexagonal boron nitride, transition metal dichalcogenides, etc. have attracted a lot of attention recently [1–5]. Although for incommensurate moiré structures in-plane translation symmetry is broken, in the long-wavelength limit and when the moiré potential is weak, one can still adopt a momentum-space description of the low-energy electronic states [6–8]. In this context, Bistritzer and MacDonald first found that the moiré structure formed by twisted bilayer graphene has flat bands at charge neutrality for certain "magic angles" of twisting [8]. The strongly suppressed kinetic energy in these flat bands suggests potential for interaction-driven exotic phases, which were recently revealed experimentally in Refs. [9–11], where both correlated insulating and unconventional superconducting ($T_c \sim 1$K) phases were found near charge neutrality in twisted bilayer graphene at the first magic angle $\theta \approx 1.05°$.

While the flat moiré bands in the family of twisted multilayer van der Waals materials [12–14] may host other interaction-driven phases, these phases will inevitably be restricted or selected by the symmetries of the moiré structures, which determine the form of interactions in the moiré bands [15–28]. The spatial symmetry of a moiré structure, however, cannot be easily changed since it is dictated by the crystal symmetry of the constituent layers. One main task of this paper is to provide practical ways of realizing 2D flat bands with different crystalline symmetries by design, *not* relying on moiré structures, thus enabling exploration of exotic phases in a larger parameter space. Our main idea is to replace the moiré potential [29–31] by periodic external magnetic fields or other artificial crystal potentials such as Zeeman or strain fields [32–35], that can now be created and controlled experimentally.

There has been a long effort of creating spatially periodic electric and magnetic fields and studying their influence on condensed matter systems. One of the earliest examples is the observation of Weiss oscillations in conventional two-dimensional electron gas (2DEG) in GaAs/AlGaAs subject to a one-dimensional periodic static electric potential, created by parallel fringes or metallic strip arrays, and a perpendicular homogeneous magnetic field [36], which is due to the commensuration between the cyclotron radius and the period of the electric potential [37–40]. 2D periodic electric potentials on 2DEG [41–45], with different symmetries [46–48], were also realized. In parallel, spatially periodic (orbital) magnetic fields in 1D [49–52], 2D [53–56], and Zeeman fields [57] have been experimentally realized using periodic arrays of superconducting or ferromagnetic strips or dots. More recently, 1D [58] and 2D [59–61] periodic electric potentials have also been realized in graphene.

In this work, we propose that 2D-periodic magnetic fields with zero average, applied on either 2D Dirac systems or ordinary 2DEG, are an effective and versatile way of creating flat bands with different superlattice symmetries in the low-energy electronic structure. Studies on 1D-periodic magnetic fields with zero average exist in literature [33, 62–67], but no general conclusions have been made on the existence and origin of 2D flatbands in nonquantizing 2D periodic magnetic fields. We find that for a simple 2D sinusoidal magnetic field forming a square Bravais lattice, Schrödinger (or 2DEG) and Dirac electrons exhibit drastically different behaviors in the tendency of realizing flat, low-energy bands. In particular the existence of magicness for the former is due to destructive interference reminiscent of the classic examples of flat band lattice models [68–73]. Moreover, by taking into account Zeeman coupling and spin degrees of freedom, one can naturally interpolate between Dirac and Schrödinger electrons, by varying the g-factor or the effective mass of a 2DEG. In this case we find that it is common for the lowest flat band to have a nonzero Chern

number for each spin species, despite the magnetic field having zero spatial average.

Band flattening for Dirac and Schrödinger electrons in periodic magnetic fields— We start by considering a generic 2D Dirac system subject to a perpendicular magnetic field having two cosinusoidal components along x and y directions, respectively: $\mathbf{B} = B[\cos(Kx) + \cos(Ky)]\hat{z}$, where $K \equiv 2\pi/a$ is the wave number with a the period of the magnetic modulation. Specific material realizations and effects of more complex functional forms of fields will be addressed in *Discussion*. The single-particle Hamiltonian is $H^D = v_F \boldsymbol{\sigma} \cdot \mathbf{\Pi}$, where v_F is the Fermi velocity of the Dirac electron, $\mathbf{\Pi} = -i\hbar\nabla + e\mathbf{A}$ is the kinetic momentum, and $\boldsymbol{\sigma} = \sigma_x\hat{x} + \sigma_y\hat{y}$. The vector potential $\mathbf{A}$ corresponding to the periodic magnetic field in the Coulomb gauge is

$$\mathbf{A} = \frac{B}{K}\left[-\sin(Ky)\hat{x} + \sin(Kx)\hat{y}\right]. \tag{1}$$

For such a simple vector potential it is convenient to use plane wave expansion to solve the eigenvalue problem [8] (see Supplemental Information). The momentum space Hamiltonian has a single dimensionless parameter $\phi \equiv eB/\hbar K^2$ determining the strength of the magnetic potential. We have used a momentum cutoff of the form $\max(|K_x|, |K_y|) \leq K_c$, where $\mathbf{K}$ labels reciprocal lattice vectors and found that convergence [8, 74] for moderate values of $\phi \sim 1$ can be well achieved with $K_c = 5$.

The Dirac Hamiltonian with the periodic vector potential Eq. (1) has a particle-hole symmetry: $\sigma_z H^D \sigma_z = -H^D$ and a zero energy solution. By diagonalizing the truncated Hamiltonian and focusing on the two particle-hole symmetric bands near zero energy we found that the velocity near zero momentum monotonically decreases with increasing ϕ, and approaches zero asymptotically, as shown in Fig. 1 (a,b). Moreover, the overall band widths of the two low-energy bands are also monotonically decreasing [75], consistent with the behavior at small momentum. Thus one can get as flat as possible low-energy bands by keeping increasing ϕ without fine-tuning. We also note that the renormalized Fermi velocity near zero momentum can be obtained analytically by perturbing the zero-energy eigen solution of H^D with $\hbar v_F \boldsymbol{\sigma} \cdot \mathbf{k}$ [75–77]. This gives $v_F^{\text{eff}} = v_F/[I_0(2\phi)]^2$, where I_0 is the zeroth modified Bessel function of the first kind. Importantly, the flatness is controlled by $\phi = eB/\hbar K^2$ instead of B alone, which can be large by having a large period even with a relatively small B. Quantitative estimates, including lower bounds on the magnetic field set by disorder potential, will be given in *Discussion*.

For a triangular lattice periodic magnetic field, our calculation shows that the band flattening behavior is qualitatively the same as the square lattice case [75]. Thus periodic magnetic fields can be used as an effective way of creating flat band Dirac systems with different superlattice symmetries.

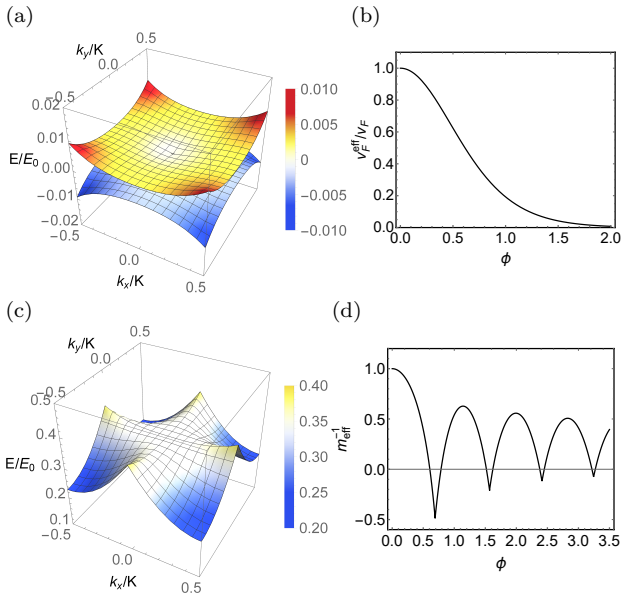

FIG. 1. Flat bands for Dirac electrons (a,b) and 2DEG (c,d) in periodic magnetic fields. (a) Band structure for the two particle-hole symmetric bands close to zero energy when $\phi = 2$. $E_0 = \hbar v_F K$ is the energy unit. The color scale is the same as E/E_0. (b) Renormalized Fermi velocity v_F^{eff} vs. ϕ. A plane wave cutoff of $K_c = 5K$ is used. (c) Band structure for the lowest band when $\phi = 0.6$ near the first magic value. $E_0 = \hbar^2 K^2/2m$. The color scale is the same as E/E_0 with white corresponding to the energy at $\mathbf{k} = 0$. (b) Renormalized inverse effective mass m_{eff}^{-1} (in units of m^{-1}) vs. ϕ. The cutoff is $K_c = 9K$.

Another consequence of the flat band, in addition to enhancing correlation effects, is the immobility of the wavepacket centered around $\mathbf{k} = 0$. Physically it means that particles described by such wavepackets will be easily trapped or localized by disorder. This is formally considered as the homogenization problem in PDE theory, which absorbs the effect of a periodic potential into an effective mass tensor by considering the dynamics at a much larger scale than the period. There is a large literature on the subject in the Schrödinger case, see e.g., Refs. [78, 79] for some rigorous mathematical references. The situation is similar for the Dirac equation under appropriate assumptions, which will be addressed in a future work [80]. In this context the vanishing v_F^{eff} directly corresponds to flat bands for the Dirac operator.

We next show that periodic magnetic fields can lead to flat bands for 2D Schrödinger electrons, but only at discrete values of the parameter ϕ. Using the same vector potential Eq. (1), the Hamiltonian is $H^S = \frac{1}{2m}\mathbf{\Pi}^2$, where m is the effective mass. By diagonalizing the momentum space Hamiltonian with a large enough cutoff, we calculate the inverse effective mass of the lowest band m_{eff}^{-1} at $\mathbf{k} = 0$ and plot it against ϕ. Fig. 1 (d) shows that m_{eff}^{-1} has an oscillatory dependence on ϕ and crosses zero repeatedly as ϕ increases. In [75] we show that al-

though the band width of the lowest band is nonzero when $m_{\rm eff}^{-1}(\mathbf{k}=0)$ vanishes, it reaches local minima at these points, accompanied by diverging density of states at the energy of the lowest band at $\mathbf{k}=0$. In the more generalized context mentioned above it is still reasonable to be called flat bands at these magic values.

Our real space calculation using the spectral method [75] gives the same result. Our calculations for a triangular lattice periodic magnetic field also show similar oscillatory behavior [75]. Later in *Discussion* we will show that the qualitative behavior is retained even for more realistic Gaussian-like magnetic field profile. Thus in contrast to Dirac electrons, 2DEG can have flat bands with exact vanishing of $m_{\rm eff}^{-1}$ at magic values of ϕ. However, to understand the origin of the recurring magic values in the Schrödinger case and why there is no magicness in the Dirac case, we have to look into details of the wavefunctions associated with the flat bands.

Wannier functions of the flat bands and minimal tight-binding models— We next examine the Wannier functions associated with the lowest bands for both 2DEG and Dirac electrons, and based on them explain the contrasting band flattening behaviors using minimal tight-binding models.

For the 2DEG case, we found that the absolute value of the maximally localized Wannier function (MLWF) [81] of the lowest band has four peaks at $\pm\frac{\pi}{K}\hat{x}$ and $\pm\frac{\pi}{K}\hat{y}$, which are minima of $|\mathbf{A}|^2$ [75]. This suggests that it may be possible to use a basis of two Gaussian-like Wannier functions, located at the plaquette corners $(\pi/K,0)$ and $(0,\pi/K)$ to describe the lowest band. In [75] we show that this is indeed the case and the resulting two-orbital tight-binding model reproduces the two lowest bands from the plane wave calculation very well. More importantly, the tight-binding Hamiltonian has complex hopping parameters and the nearest-neighbor hopping is almost purely imaginary near the first magic value of ϕ. These features provide important clues for our construction of a minimal tight-binding model below.

For the Dirac case, we make use of the particle-hole symmetry of the Hamiltonian H^D and consider its square $(H^D)^2$ [75]. In stark contrast to the Schrödinger case, the peaks of the MLWF of the lowest band are now located at $(\pm\pi/K,\pm\pi/K)$ (four equivalent points) and $(0,0)$, which are the minima of $\pm B(\mathbf{r})$ for spin up and down, respectively [75]. Thus the tight-binding Hamiltonian for each spin is one-dimensional, and all the hopping parameters are real and monotonically decrease as ϕ increases. This is because the potential wells of $\pm B(\mathbf{r})$ become monotonically deeper.

The Wannier functions obtained above motivate us to construct minimal tight-binding models to explain the different behaviors of 2DEG and Dirac electrons. For 2DEG, we consider a model with spinless free fermions hopping between nearest neighbors on a 2D square lattice, where the lattice sites coincide with the plaquette corners:

$$H=-\sum_{\langle ij\rangle} te^{i\varphi_{ij}}c_i^\dagger c_j+4t, \tag{2}$$

where $t=\hbar^2/2ma^2$ is the hopping parameter between nearest neighbors, and the summation is over nearest neighbors. For the 2D-cosinusoidal magnetic field used above the absolute value of the flux through a plaquette is $\Phi=16B/K^2=8Ba^2/\pi^2$. All positive flux plaquettes only share edges with negative flux ones [Fig. 2 (a)]. The magnetic field is included as a Peierls phase in the hopping parameter, motivated by the shape of the complex Wannier functions [75]. The vector potential Eq. (1) leads to $\varphi_{ij}=\pm\frac{4eB}{\hbar K^2}=\pm\frac{\pi\Phi}{2\Phi_0}=\pm 4\phi$, where positive sign means the plaquette on the left of the directional hopping path has positive flux, and $\Phi_0=h/e$.

The momentum space Hamiltonian can be easily diagonalized[75]. Expanding the eigenenergies at small k, one finds a series of magic values at which the inverse effective mass vanishes:

$$\phi=\frac{(2n+1)\pi}{8},\ n\in\mathbb{Z}, \tag{3}$$

with the periodicity $\Delta\phi=\pi/4\approx 0.785$, which is close to the period of the oscillation in Fig. 1 (d). The model fails, however, to capture some fine features in the plane wave results, e.g., the negative values of $m_{\rm eff}^{-1}$ near the magic values, the decreasing amplitudes of the oscillation with increasing ϕ, etc., which is not surprising given the simplicity of the model. Nonetheless, the model helps to elucidate the origin of the magicness, which is the destructive interference of different hopping terms, similar to many early examples of flat band lattice models [68–73]. In the present case, the destructive interference comes from the values of ϕ in Eq. (3), at which $t_{ij}=-t_{ji}$ for nearest neighbors i and j. Specifically, for some local wavefunction having equal weights on two diagonal sites of a plaquette, which belong to the same sublattice, hopping to their common nearest neighbors will cancel out. This is the reason for the complete flatness of the bands along $k_x=\pm k_y$. At distances much larger than the lattice period, such cancellation leads to strong suppression of hopping along almost all directions, which is the reason for the vanishing inverse effective mass near $\mathbf{k}=0$.

In contrast, the minimal model for the Dirac case [more exactly for $(H^D)^2$] is trivial, which is a nearest-neighbor hopping model on a square lattice with one site per unit cell. Such a model obviously cannot describe the band flattening as it stands, unless one allows the hopping amplitude to depend on ϕ which is *a posteriori*. Physically, the decreasing hopping with increasing ϕ should have two origins. The first is the Landau localization in the strong field limit. The second, which is unique to Dirac electrons, is the localization due to the Zeeman potential in $(H^D)^2$ which has a Berry phase origin.

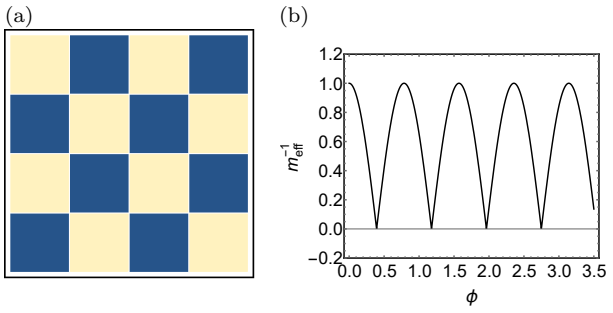

FIG. 2. (a) Tight-binding model on a square lattice with staggered magnetic fields for 2DEG. The xy axes are rotated by $\pi/4$ compared to that used for Eq. (1). (b) Inverse effective mass versus ϕ.

Zeeman coupling and flat band Chern insulators— We now consider the Zeeman coupling between 2DEG and the periodic magnetic field, which always accompanies the orbital coupling. In particular, Dirac electrons (based on the squared Hamiltonian) can be viewed as a special case of 2DEG plus Zeeman coupling with $gm/m_e = 2$, where g is the g-factor, m is the effective mass of the 2DEG, and m_e is the free electron mass. In common 2DEGs this ratio can vary significantly depending on materials realization [82, 83] and may even be tunable in a given system [57, 84, 85]. We thus take the Zeeman coupling strength gm/m_e as a variable and study how the flat band behaviors of 2DEG and Dirac electrons can be smoothly bridged by changing it between 0 and 2.

Figure 3 (a) shows the phase diagram of the inverse effective mass $m_{\rm eff}^{-1}$ (in units of m^{-1}) at $\mathbf{k} = 0$ versus ϕ and gm/m_e. One can see that along the horizontal line of $gm/m_e = 0$, i.e., 2DEG without Zeeman coupling, $m_{\rm eff}^{-1}$ oscillates between positive (red color) and negative (blue color) values, and reaches 0 (white color) at magic values of ϕ. This is basically the same as Fig. 1 (d). Similarly when $gm/m_e = 2$ the figure reproduces the monotonic decay of $m_{\rm eff}^{-1}$ for the Dirac case shown in Fig. 1 (d). In between these two limits the regions with negative $m_{\rm eff}^{-1}$ form bands which start from being perpendicular to the ϕ axis when $gm/m_e = 0$, and gradually bend toward the horizontal $gm/m_e = 2$ line as gm/m_e increases. Accordingly, the lines of magic values of ϕ and gm/m_e, defined by $m_{\rm eff}^{-1} = 0$, also bend to $gm/m_e = 2$ and disappear from the field of view.

In [75], we have constructed a minimal 3-band model, based on the Wannier functions, to qualitatively capture the band flattening behavior for general values of gm/m_e. Interestingly, we find that the lowest band of the model quite generally has a nonzero Chern number, making it similar to the Haldane model of quantum anomalous Hall effect with zero net magnetic field [86], but on the square lattice instead of the honeycomb lattice. We thus calculate the Chern number of the lowest-band $\mathcal{C}_1$ using the plane wave method [75] in a 2D parameter space spanned by ϕ and gm/m_e, which is shown in Fig. 3 (b). One can see that the Chern insulator phase is ubiquitous. Most regions have a $\mathcal{C}_1 = -1$ while on several narrow bands it is $+1$. These regions are separated by lines corresponding to band touching where the Chern number is ill-defined. Comparing Figs. 3 (a) and (b), one can see that the $\mathcal{C}_1 = 1$ regions coincide with places where $m_{\rm eff}^{-1}$ is extremal, indicating that there is band inversion near these values of $m_{\rm eff}^{-1}$. Most importantly, the regions with zero or vanishingly small $m_{\rm eff}^{-1}$ almost all have nonzero $\mathcal{C}_1$. Thus by tuning to the magic values of ϕ and gm/m_e one could have flat bands and nontrivial topology simultaneously.

For the simple 2DEG Hamiltonian used here, all bands have two-fold degeneracy due to an emergent symmetry of the bipartite lattice. The nonzero Chern number above should thus be understood as a spin Chern number. To get nonzero charge Chern numbers one simply needs to lift this effective Kramers degeneracy, by e.g. adding a periodic scalar potential commensurate with the periodic magnetic field.

Discussion— The magnetic field used above has a very simple form [49–52]. In reality magnetic fields created by periodic arrays of bar magnets or superconducting wires will have more Fourier components, as well as finite in-plane magnetic fields. However, on the one hand the sinusoidal potential can be viewed as a legitimate first approximation if the spatial profile of the magnetic field is smooth [49–52]. On the other hand, we expect the general low-energy behavior of Dirac electrons or 2DEG revealed in this work to qualitatively hold even with more realistic potential profiles, including that due to the pseudomagnetic fields created by strain in graphene [35, 87–89]. To prove this we have performed calculations for periodic Gaussian magnetic fields (for 2DEG) and periodic Gaussian strain fields (for Dirac electrons) [87–89] (Fig. 3 in [75]) using the spectral method. The results strongly resemble those for the simple cosinusoidal fields. Namely, in the Dirac case the velocity monotonically decreases, while in the Schrödinger case the inverse effective

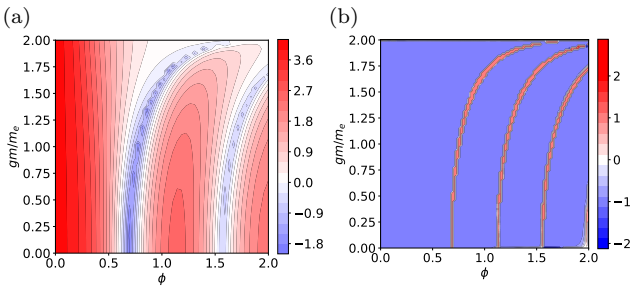

FIG. 3. (a) Inverse effective mass at $\mathbf{k} = 0$ and (b) Chern number of the up spin for the lowest band versus gm/m_e and ϕ. $K_c = 5K$. Brillouin zone discretization of 11×11 and 10×10 were used for calculating $m_{\rm eff}^{-1}$ and Chern number, respectively.

mass repeatedly crosses zero.

The typical strength of fields needed to get flat bands should be such that the magnetic flux through each plaquette is on the order of Φ_0. We emphasize that this is a rather modest requirement (see below) especially for large periods or small K. Since $\Phi_0 \approx 4.136\times10^{-3}$ T$\cdot\mu$m^2, a μm period field only needs to have an amplitude $\sim 10^2$ Gauss. In the case of graphene, such long wavelengths also mean the two valleys of graphene can be viewed as independent [90, 91]. Based on the lessons learned from the twisted multilayer graphene systems, for interaction-driven phases to appear the number of moiré unit cells in a given sample does not have to be macroscopically large– $10^2 \times 10^2$ is sufficient. Artificial superlattices with such number of periods are not out of reach [49, 50, 54–57]. Experimentally one can use either transport [54–56, 59–61] or spectroscopic [90] methods to reveal the existence of the flat bands [9, 10, 12, 13] and in addition to look for exotic phases at very low temperatures.

Disorder places another constraint on the lower bound of the magnetic field or the upper bound of the spatial period. For the Bloch wave picture to be valid, the kinetic energy of the electron must be larger than the disorder potential Γ. Thus for a given spatial period $2\pi/K$, the width of the band under discussion must be at least larger than the disorder potential. This requires $\hbar^2K^2/2m > \Gamma$ for 2DEG and $\hbar v_F K > \Gamma$ for Dirac electrons, and consequently gives a lower bound of the magnetic field if $\phi \sim 1$. For Dirac electrons, in the case of graphene, $\Gamma \sim 1$ meV if we adopt the experimental relaxation time of 3.0×10^{-13}s [92]. Thus $K \geq 1.67 \times 10^{-3}$nm^{-1}, or the period must be smaller than 3.8 μm, and $B \geq 3.7$ mT for achieving nearly flat bands ($\phi \sim 2$). For high mobility 2DEG such as GaAs/AlGaAs, $\Gamma \sim 0.01$ meV if using the mobility μ =70 m^2/(V$\cdot$s) [93] and the effective mass 0.067 m_e. This corresponds to a lower bound $K \geq 4.6\times10^{-3}$ nm^{-1} (or a period of 1.4 μm), and $B \geq 8.6$ mT for achieving nearly flat bands ($\phi \sim 0.6$). These values of B are at least one order of magnitude smaller than that achieved experimentally for smooth spatial modulations of real magnetic field [49, 50, 94–98] or strain [35, 87–89], and the micrometer period is also experimentally realizable [49, 50, 94–98].

While our prescription works for the whole spectrum bridging Dirac materials and 2DEG, the former can take advantage of the various pseudo-magnetic fields through e.g. periodic strain or Zeeman field that may be easier to implement experimentally. Moreover, practically the absence of "magicness" in the Dirac case makes it much easier to realize flat bands without the need of fine tuning. On the other hand, the complex hopping in the tight-binding model for 2DEG is reminiscent of the loop-current model for cuprates [99, 100], thus suggesting potential new phases more proximate to high-temperature superconductors on a square lattice.

MT and HC were supported by the start-up funding of CSU. OP is supported by NSF CAREER grant DMS-1452349. The authors are grateful to Allan MacDonald, Qian Niu, Di Xiao, Francois Peeters, and Pablo Jarillo-Herrero for helpful discussions.

[1] J. Hass, F. Varchon, J. E. Millán-Otoya, M. Sprinkle, N. Sharma, W. A. de Heer, C. Berger, P. N. First, L. Magaud, and E. H. Conrad, Phys. Rev. Lett. **100**, 125504 (2008).
[2] C. R. Dean, A. F. Young, I. Meric, C. Lee, L. Wang, S. Sorgenfrei, K. Watanabe, T. Taniguchi, P. Kim, K. L. J. Shepard, and J. Hone, Nature Nanotechnology **5**, 722 (2010).
[3] J. Xue, J. Sanchez-Yamagishi, D. Bulmash, P. Jacquod, A. Deshpande, K. Watanabe, T. Taniguchi, P. Jarillo-Herrero, and B. J. LeRoy, Nature Materials **10**, 282 (2011).
[4] E. Wang, X. Lu, S. Ding, W. Yao, M. Yan, G. Wan, K. Deng, S. Wang, G. Chen, L. Ma, J. Jung, A. V. Fedorov, Y. Zhang, G. Zhang, and S. Zhou, Nature Physics **12**, 1111 (2016).
[5] C. Zhang, C.-P. Chuu, X. Ren, M.-Y. Li, L.-J. Li, C. Jin, M.-Y. Chou, and C.-K. Shih, Science Advances **3**, e1601459 (2017).
[6] J. M. B. Lopes dos Santos, N. M. R. Peres, and A. H. Castro Neto, Phys. Rev. Lett. **99**, 256802 (2007).
[7] E. J. Mele, Phys. Rev. B **81**, 161405 (2010).
[8] R. Bistritzer and A. H. MacDonald, PNAS **108**, 12233 (2011).
[9] Y. Cao, V. Fatemi, A. Demir, S. Fang, S. L. Tomarken, J. Y. Luo, J. D. Sanchez-Yamagishi, K. Watanabe, T. Taniguchi, E. Kaxiras, R. C. Ashoori, and P. Jarillo-Herrero, Nature **556**, 80 (2018).
[10] Y. Cao, V. Fatemi, S. Fang, K. Watanabe, T. Taniguchi, E. Kaxiras, and P. Jarillo-Herrero, Nature **556**, 43 (2018).
[11] M. Yankowitz, S. Chen, H. Polshyn, Y. Zhang, K. Watanabe, T. Taniguchi, D. Graf, A. F. Young, and C. R. Dean, Science **363**, 1059 (2019).
[12] D. Pierucci, H. Sediri, M. Hajlaoui, J.-C. Girard, T. Brumme, M. Calandra, E. Velez-Fort, G. Patriarche, M. G. Silly, G. Ferro, V. Soulire, M. Marangolo, F. Sirotti, F. Mauri, and A. Ouerghi, ACS Nano **9**, 5432 (2015).
[13] B. L. Chittari, G. Chen, Y. Zhang, F. Wang, and J. Jung, Phys. Rev. Lett. **122**, 016401 (2019).
[14] G. E. Volovik, JETP Letters **107**, 516 (2018).
[15] C. Xu and L. Balents, Phys. Rev. Lett. **121**, 087001 (2018).
[16] A. M. DaSilva, J. Jung, and A. H. MacDonald, Phys. Rev. Lett. **117**, 036802 (2016).
[17] G. Baskaran, arXiv:1804.00627 (2018).
[18] J. F. Dodaro, S. A. Kivelson, Y. Schattner, X. Q. Sun, and C. Wang, Phys. Rev. B **98**, 075154 (2018).
[19] J. González and T. Stauber, Phys. Rev. Lett. **122**, 026801 (2019).
[20] H. Guo, X. Zhu, S. Feng, and R. T. Scalettar, Phys. Rev. B **97**, 235453 (2018).
[21] E. Laksonoa, J. N. Leawa, A. Reavesc, M. Singhc, X. Wanga, S. Adama, and X. Gu, Solid State Com-

munications **282**, 38 (2018).
[22] C.-C. Liu, L.-D. Zhang, W.-Q. Chen, and F. Yang, Phys. Rev. Lett. **121**, 217001 (2018).
[23] H. C. Po, L. Zou, A. Vishwanath, and T. Senthil, Phys. Rev. X **8**, 031089 (2018).
[24] S. Ray, J. Jung, and T. Das, Phys. Rev. B **99**, 134515 (2019).
[25] A. Thomson, S. Chatterjee, S. Sachdev, and M. S. Scheurer, Phys. Rev. B **98**, 075109 (2018).
[26] F. Wu, A. H. MacDonald, and I. Martin, Phys. Rev. Lett. **121**, 257001 (2018).
[27] X. Y. Xu, K. T. Law, and P. A. Lee, Phys. Rev. B **98**, 121406 (2018).
[28] N. F. Q. Yuan and L. Fu, Phys. Rev. B **98**, 045103 (2018).
[29] P. San-Jose, J. González, and F. Guinea, Phys. Rev. Lett. **108**, 216802 (2012).
[30] L.-J. Yin, J.-B. Qiao, W.-J. Zuo, W.-T. Li, and L. He, Phys. Rev. B **92**, 081406 (2015).
[31] J. González, Phys. Rev. B **94**, 165401 (2016).
[32] N. Levy, S. A. Burke, K. L. Meaker, M. Panlasigui, A. Zettl, F. Guinea, A. H. C. Neto, and M. F. Crommie, Science **329**, 544 (2010).
[33] E. Tang and L. Fu, Nature Physics **10**, 964 (2014).
[34] M. A. Mueed, M. S. Hossain, I. Jo, L. N. Pfeiffer, K. W. West, K. W. Baldwin, and M. Shayegan, Phys. Rev. Lett. **121**, 036802 (2018).
[35] Y. Jiang, M. Andelkovic, S. P. Milovanovic, L. Covaci, X. Lai, Y. Cao, K. Watanabe, T. Taniguchi, F. M. Peeters, A. K. Geim, and E. Y. Andrei, arXiv:1904.10147v1 (2019).
[36] D. Weiss, K. V. Klitzing, K. Ploog, and G. Weimann, Europhysics Letters **8**, 179 (1989).
[37] R. R. Gerhardts, D. Weiss, and K. v. Klitzing, Phys. Rev. Lett. **62**, 1173 (1989).
[38] R. W. Winkler, J. P. Kotthaus, and K. Ploog, Phys. Rev. Lett. **62**, 1177 (1989).
[39] C. W. J. Beenakker, Phys. Rev. Lett. **62**, 2020 (1989).
[40] P. Vasilopoulos and F. M. Peeters, Phys. Rev. Lett. **63**, 2120 (1989).
[41] R. R. Gerhardts, D. Weiss, and U. Wulf, Phys. Rev. B **43**, 5192 (1991).
[42] C. Albrecht, J. H. Smet, K. von Klitzing, D. Weiss, V. Umansky, and H. Schweizer, Phys. Rev. Lett. **86**, 147 (2001).
[43] M. C. Geisler, J. H. Smet, V. Umansky, K. von Klitzing, B. Naundorf, R. Ketzmerick, and H. Schweizer, Phys. Rev. Lett. **92**, 256801 (2004).
[44] X. F. Wang, P. Vasilopoulos, and F. M. Peeters, Phys. Rev. B **69**, 035331 (2004).
[45] C. Albrecht, J. H. Smet, D. Weiss, K. von Klitzing, R. Hennig, M. Langenbuch, M. Suhrke, U. Rössler, V. Umansky, and H. Schweizer, Phys. Rev. Lett. **83**, 2234 (1999).
[46] S. Chowdhury, C. J. Emeleus, B. Milton, E. Skuras, A. R. Long, J. H. Davies, G. Pennelli, and C. R. Stanley, Phys. Rev. B **62**, R4821 (2000).
[47] S. Chowdhury, A. R. Long, E. Skuras, J. H. Davies, K. Lister, G. Pennelli, and C. R. Stanley, Phys. Rev. B **69**, 035330 (2004).
[48] Y. Kato, A. Endo, S. Katsumoto, and Y. Iye, Phys. Rev. B **86**, 235315 (2012).
[49] H. A. Carmona, A. K. Geim, A. Nogaret, P. C. Main, T. J. Foster, M. Henini, S. P. Beaumont, and M. G. Blamire, Phys. Rev. Lett. **74**, 3009 (1995).
[50] P. D. Ye, D. Weiss, R. R. Gerhardts, M. Seeger, K. von Klitzing, K. Eberl, and H. Nickel, Phys. Rev. Lett. **74**, 3013 (1995).
[51] D. P. Xue and G. Xiao, Phys. Rev. B **45**, 5986 (1992).
[52] F. M. Peeters and P. Vasilopoulos, Phys. Rev. B **47**, 1466 (1993).
[53] M. C. Chang and Q. Niu, Phys. Rev. B **50**, 10843 (1994).
[54] P. D. Ye, D. Weiss, K. v. Klitzing, and K. Eberl, Appl. Phys. Lett. **67**, 1441 (1995).
[55] P. D. Ye, D. Weiss, and R. R. Gerhardts, Journal of Applied Physics **81**, 5444 (1997).
[56] E. Skuras, A. R. Long, S. Chowdhury, and M. Rahman, Journal of Applied Physics **90**, 2623 (2001).
[57] C. Betthausen, T. Dollinger, H. Saarikoski, V. Kolkovsky, G. Karczewski, T. Wojtowicz, K. Richter, and D. Weiss, Science **337**, 324 (2012).
[58] M. Drienovsky, J. Joachimsmeyer, A. Sandner, M.-H. Liu, T. Taniguchi, K. Watanabe, K. Richter, D. Weiss, and J. Eroms, Phys. Rev. Lett. **121**, 026806 (2018).
[59] L. A. Ponomarenko, R. V. Gorbachev, G. L. Yu, D. C. Elias, R. Jalil, A. A. Patel, A. Mishchenko, A. S. Mayorov, C. R. Woods, J. R. Wallbank, M. Mucha-Kruczynski, B. A. Piot, M. Potemski, I. V. Grigorieva, K. S. Novoselov, F. Guinea, V. I. Falko, and A. K. Geim, Nature **497**, 594 (2013).
[60] C. R. Dean, L. Wang, P. Maher, C. Forsythe, F. Ghahari, Y. Gao, J. Katoch, M. Ishigami, P. Moon, M. Koshino, T. Taniguchi, K. Watanabe, K. L. Shepard, J. Hone, and P. Kim, Nature **497**, 598 (2013).
[61] R. K. Kumar, A. Mishchenko, X. Chen, S. Pezzini, G. H. Auton, L. A. Ponomarenko, U. Zeitler, L. Eaves, V. I. Falko, and A. K. Geim, PNAS **115**, 5135 (2018).
[62] I. S. Ibrahim and F. M. Peeters, Phys. Rev. B **52**, 17321 (1995).
[63] Y. H. Chiu, Y. H. Lai, J. H. Ho, D. S. Chuu, and M. F. Lin, Phys. Rev. B **77**, 045407 (2008).
[64] L. Dell'Anna and A. De Martino, Phys. Rev. B **79**, 045420 (2009).
[65] M. R. Masir, P. Vasilopoulos, and F. M. Peeters, New Journal of Physics **11**, 095009 (2009).
[66] L. Z. Tan, C.-H. Park, and S. G. Louie, Phys. Rev. B **81**, 195426 (2010).
[67] M. Taillefumier, V. K. Dugaev, B. Canals, C. Lacroix, and P. Bruno, Phys. Rev. B **84**, 085427 (2011).
[68] B. Sutherland, Phys. Rev. B **34**, 5208 (1986).
[69] E. H. Lieb, Phys. Rev. Lett. **62**, 1201 (1989).
[70] A. Mielke, Journal of Physics A: Mathematical and General **24**, L73 (1991).
[71] A. Mielke, Journal of Physics A: Mathematical and General **24**, 3311 (1991).
[72] H. Tasaki, Phys. Rev. Lett. **69**, 1608 (1992).
[73] H. Tasaki, Eur. Phys. J. B **64**, 365 (2008).
[74] J. M. B. Lopes dos Santos, N. M. R. Peres, and A. H. Castro Neto, Phys. Rev. B **86**, 155449 (2012).
[75] Supplemental Information.
[76] R. Jackiw, Phys. Rev. D **29**, 2375 (1984).
[77] I. Snyman, Phys. Rev. B **80**, 054303 (2009).
[78] G. Allaire and A. Piatnitski, Communications in Mathematical Physics **258**, 1 (2005).
[79] L. Barletti and N. Ben Abdallah, Communications in Mathematical Physics **307**, 567 (2011).
[80] H. Chen, O. Pinaud, and M. Tahir, in preparation.
[81] N. Marzari and D. Vanderbilt, Phys. Rev. B **56**, 12847

(1997).
[82] S. Adachi, J. Appl. Phys. **53**, 8775 (1982).
[83] A. A. Taskin and Y. Ando, Phys. Rev. B **84**, 035301 (2011).
[84] A. Giorgioni, S. Paleari, S. Cecchi, E. Vitiello, E. Grilli, G. Isella, W. Jantsch, M. Fanciulli, and F. Pezzoli, Nature Communications **7**, 13886 (2016).
[85] Z. Wang, Z. Zhong, X. Hao, S. Gerhold, B. Stöger, M. Schmid, J. Sánchez-Barriga, A. Varykhalov, C. Franchini, K. Held, and U. Diebold, Proc. Natl. Acad. Sci. **111**, 3933 (2014).
[86] F. D. M. Haldane, Phys. Rev. Lett. **61**, 2015 (1988).
[87] A. H. Castro Neto, F. Guinea, N. M. R. Peres, K. S. Novoselov, and A. K. Geim, Rev. Mod. Phys. **81**, 109 (2009).
[88] F. Guinea, M. I. Katsnelson, and A. K. Geim, Nature Physics **6**, 30 (2010).
[89] D. Zhai and N. Sandler, Modern Physics Letters B **33**, 1930001 (2019).
[90] M. Yankowitz, J. Xue, D. Cormode, J. D. Sanchez-Yamagishi, K. Watanabe, T. Taniguchi, P. Jarillo-Herrero, P. Jacquod, and B. J. LeRoy, Nature Physics **8**, 382 (2012).
[91] C.-H. Park, L. Yang, Y.-W. Son, M. L. Cohen, and S. G. Louie, Nature Physics **4**, 213 (2008).
[92] T. Stauber, N. M. R. Peres, and F. Guinea, Phys. Rev. B **76**, 205423 (2007).
[93] A. Endo and Y. Iye, Journal of the Physical Society of Japan **77**, 064713 (2008).
[94] K. S. Novoselov, A. K. Geim, S. V. Dubonos, Y. G. Cornelissens, F. M. Peeters, and J. C. Maan, Phys. Rev. B **65**, 233312 (2002).
[95] A. Nogaret, D. N. Lawton, D. K. Maude, J. C. Portal, and M. Henini, Phys. Rev. B **67**, 165317 (2003).
[96] A. Tarasov, S. Hugger, H. Xu, M. Cerchez, T. Heinzel, I. V. Zozoulenko, U. Gasser-Szerer, D. Reuter, and A. D. Wieck, Phys. Rev. Lett. **104**, 186801 (2010).
[97] A. Nogaret, J. Phys.: Condens. Matter **22**, 253201 (2010).
[98] A. Leuschner, J. Schluck, M. Cerchez, T. Heinzel, K. Pierz, and H. W. Schumacher, Phys. Rev. B **95**, 155440 (2017).
[99] C. M. Varma, Phys. Rev. B **55**, 14554 (1997).
[100] C. M. Varma, Phys. Rev. B **73**, 155113 (2006).